ELSEVIER

J. Non-Newtonian Fluid Mech. 129 (2005) 117–127

Journal of Non-Newtonian Fluid Mechanics

www.elsevier.com/locate/jnnfm

Cessation of Couette and Poiseuille flows of a Bingham plastic and finite stopping times

Maria Chatzimina[a], Georgios C. Georgiou[a,*], Ioannis Argyropaidas[b], Evan Mitsoulis[b], R.R. Huilgol[c]

[a] *Department of Mathematics and Statistics, University of Cyprus, P.O. Box 20537, 1678 Nicosia, Cyprus*
[b] *School of Mining Engineering and Metallurgy, National Technical University of Athens, Heroon Polytechniou 9, 157 80 Zografou, Athens, Greece*
[c] *School of Informatics and Engineering, Flinders University of South Australia, G.P.O. Box 2100, Adelaide, SA 5001, Australia*

Received 20 January 2005; received in revised form 5 July 2005; accepted 5 July 2005

Abstract

We solve the one-dimensional cessation Couette and Poiseuille flows of a Bingham plastic using the regularized constitutive equation proposed by Papanastasiou and employing finite elements in space and a fully implicit scheme in time. The numerical calculations confirm previous theoretical findings that the stopping times are finite when the yield stress is nonzero. The decay of the volumetric flow rate, which is exponential in the Newtonian case, is accelerated and eventually becomes linear as the yield stress is increased. In all flows studied, the calculated stopping times are just below the theoretical upper bounds, which indicates that the latter are tight.

Keywords: Couette flow; Poiseuille flow; Bingham plastic; Papanastasiou model; Cessation

1. Introduction

In viscometric flows, one can bring a fluid to a halt by setting the moving boundary to rest in the case of Couette flows, or by reducing the applied pressure gradient to zero in Poiseuille flows. In a Newtonian fluid, the corresponding steady velocity fields decay to zero in an infinite amount of time [1]. In a Bingham plastic, the velocity fields go to zero in a finite time, which emphasizes the role of the yield stress [2,3]. Glowinski [2] and Huilgol et al. [3] have provided explicit theoretical finite upper bounds on the time for a Bingham material to come to rest in various flows, such as the plane and circular Couette flows and the plane and axisymmetric Poiseuille flows. To be specific, each upper bound depends on the density, the viscosity, the yield stress and the least eigenvalue of the Laplacian operator on the flow domain [2,3]. As for the underlying cause for the finite extinction time, it can be shown that the yield surface moves laterally with a finite speed bringing the fluid to a halt, and that kinematical conditions play a crucial role [4]. In a similar fashion, the upper bounds derived by Huilgol [5] for the cessation of axisymmetric Poiseuille flows with more general viscoplastic fluids must be caused by the lateral movement of the yield surface.

The objective of the present work is to compute numerically the stopping times and make comparisons with the theoretical upper bounds provided in the literature for the cessation of three flows of a Bingham fluid: (a) the plane Couette flow; (b) the plane Poiseuille flow; (c) the axisymmetric Poiseuille flow. Instead of the ideal Bingham-plastic constitutive equation, we employ the regularized equation proposed by Papanastasiou [6], to avoid the determination of the yielded and unyielded regions in the flow domain. It should be noted that preliminary results for the case of the plane Poiseuille flow can also be found in Ref. [7].

The paper is organized as follows. In Section 2, we discuss the regularized Papanastasiou equation for a Bingham plastic. In Section 3, we present the dimensionless forms of the governing equations for the three flows of interest along with the corresponding theoretical upper bounds. In Section 4, we present and discuss representative numerical results for all flows. The numerical stopping times are just below

* Corresponding author. Tel.: +357 22892612; fax: +357 22892601.
E-mail address: georgios@ucy.ac.cy (G.C. Georgiou).

0377-0257/$ – see front matter © 2005 Elsevier B.V. All rights reserved.
doi:10.1016/j.jnnfm.2005.07.001

the theoretical upper bounds, i.e. the latter are tight. Some discrepancies are observed only for low Bingham numbers when the growth parameter in the Papanastasiou model is not sufficiently high. Finally, Section 5 contains the conclusions of this work.

2. Constitutive equation

Let $\mathbf{u}$ and $\boldsymbol{\tau}$ denote the velocity vector and the stress tensor, respectively, and $\dot{\boldsymbol{\gamma}}$ denote the rate-of-strain tensor,

$$\dot{\boldsymbol{\gamma}} \equiv \nabla\mathbf{u} + (\nabla\mathbf{u})^{\mathrm{T}}, \tag{1}$$

where $\nabla\mathbf{u}$ is the velocity-gradient tensor, and the superscript T denotes its transpose. The magnitudes of $\dot{\boldsymbol{\gamma}}$ and $\boldsymbol{\tau}$ are respectively defined as follows:

$$\dot{\gamma} = \sqrt{\frac{1}{2}\mathrm{II}_{\dot{\boldsymbol{\gamma}}}} = \sqrt{\frac{1}{2}\dot{\boldsymbol{\gamma}} : \dot{\boldsymbol{\gamma}}} \quad \text{and} \quad \tau = \sqrt{\frac{1}{2}\mathrm{II}_{\boldsymbol{\tau}}} = \sqrt{\frac{1}{2}\boldsymbol{\tau} : \boldsymbol{\tau}}, \tag{2}$$

where II stands for the second invariant of a tensor.

In tensorial form, the Bingham model is written as follows:

$$\begin{cases} \dot{\boldsymbol{\gamma}} = \mathbf{0}, & \tau \le \tau_0, \\ \boldsymbol{\tau} = \left(\frac{\tau_0}{\dot{\gamma}} + \mu\right)\dot{\boldsymbol{\gamma}}, & \tau \ge \tau_0, \end{cases} \tag{3}$$

where τ_0 is the yield stress, and μ is a constant viscosity.

In any flow of a Bingham plastic, determination of the yielded ($\tau \ge \tau_0$) and unyielded ($\tau \le \tau_0$) regions in the flow field is necessary, which leads to considerable computational difficulties in the use of the model. These are overcome by using the regularized constitutive equation proposed by Papanastasiou [6]:

$$\boldsymbol{\tau} = \left\{ \frac{\tau_0[1 - \exp(-m\,\dot{\gamma})]}{\dot{\gamma}} + \mu \right\} \dot{\boldsymbol{\gamma}}, \tag{4}$$

where m is a stress growth exponent. For sufficiently large values of the regularization parameter m, the Papanastasiou model provides a satisfactory approximation of the Bingham model, while at the same time the need of determining the yielded and the unyielded regions is eliminated. The model has been used with great success in solving various steady and time-dependent flows (see, for example, [8,9] and the references therein).

3. Flow problems and governing equations

The governing equations along with the boundary and initial conditions of the three time-dependent, one-dimensional Bingham-plastic flows of interest are discussed below. The theoretical upper bounds of Glowinski [2] and Huilgol et al. [3] for the stopping times are also presented.

3.1. Cessation of plane Couette flow

The geometry of the plane Couette flow is shown in Fig. 1a. The steady-state solution is given by

$$u_x^s(y) = \left(1 - \frac{y}{H}\right) V, \tag{5}$$

where V is the speed of the lower plate (the upper one is kept fixed) and H is the distance between the two plates. We assume that at $t = 0$, the velocity $u_x(y, t)$ is given by the above profile and that at $t = 0^+$ the lower plate stops moving. To nondimensionalize the x-momentum equation, we scale the lengths by H, the velocity by V, the stress components by $\mu V/H$, and the time by $\rho H^2/\mu$, where ρ is the constant density of the fluid. With these scalings, the x-momentum equation becomes

$$\frac{\partial u_x}{\partial t} = \frac{\partial \tau_{yx}}{\partial y}. \tag{6}$$

The dimensionless form of the Papanastasiou model is reduced to

$$\tau_{yx} = \left\{ \frac{Bn[1 - \exp(-M\dot{\gamma})]}{\dot{\gamma}} + 1 \right\} \frac{\partial u_x}{\partial y}, \tag{7}$$

where $\dot{\gamma} = |\partial u_x/\partial y|$,

$$Bn \equiv \frac{\tau_0 H}{\mu V} \tag{8}$$

is the Bingham number, and

$$M \equiv \frac{mV}{H} \tag{9}$$

is the dimensionless growth parameter.

The dimensionless boundary and initial conditions are as follows:

$$\begin{aligned} &u_x(0, t) = 0, \quad t > 0, \qquad u_x(1, t) = 0, \quad t \ge 0, \\ &u_x(y, 0) = 1 - y, \quad 0 \le y \le 1. \end{aligned} \tag{10}$$

In the case of a Newtonian fluid ($Bn = 0$), the analytical solution of the time-dependent flow, governed by Eqs. (6), (7) and (10), is known [1]:

$$u_x(y, t) = \frac{2}{\pi} \sum_{k=1}^{\infty} \frac{1}{k} \sin(k\pi y)\, \mathrm{e}^{-k^2\pi^2 t}. \tag{11}$$

Hence, the flow ceases theoretically in an infinite amount of time. If the fluid is a Bingham plastic ($Bn > 0$), however, the flow comes to rest in a finite amount of time, as demonstrated by Huilgol et al. [3], who provide the following upper bound for the dimensionless stopping time:

$$T_f \le \frac{4}{\pi^2} \ln\left[1 + \frac{\pi^2}{2}\frac{\|u_x(y, 0)\|}{Bn}\right], \tag{12}$$

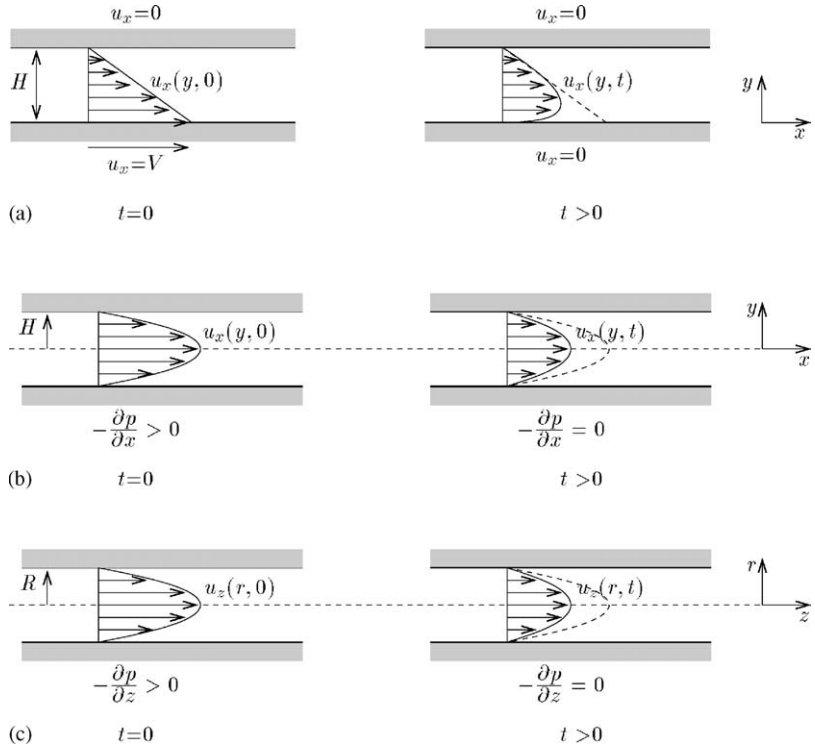

Fig. 1. Flow problems under study: (a) cessation of plane Couette flow; (b) cessation of plane Poiseuille flow; (c) cessation of axisymmetric Poiseuille flow.

where

$$\|u_x(y,0)\| = \left[\int_0^1 u_x^2(y,0)\,\mathrm{d}y\right]^{1/2}. \tag{13}$$

From Eq. (10), it is easily deduced that $\|u_x(y,0)\| = 1/\sqrt{3}$.

3.2. Cessation of plane Poiseuille flow

The geometry of the plane Poiseuille flow is depicted in Fig. 1b. The steady-state solution for the ideal (i.e. nonregularized) Bingham fluid is given by

$$u_x^s(y) = \begin{cases} \frac{1}{2\mu}\left(-\frac{\partial p}{\partial x}\right)^s (H-y_0)^2, & 0 \le y \le y_0, \\ \frac{1}{2\mu}\left(-\frac{\partial p}{\partial x}\right)^s (H^2-y^2) - \frac{\tau_0}{\mu}(H-y), & y_0 \le y \le H, \end{cases} \tag{14}$$

where $(-\partial p/\partial x)^s$ is the steady-state pressure gradient, and

$$y_0 = \frac{\tau_0}{(-\partial p/\partial x)^s} < H \tag{15}$$

denotes the point at which the material yields. Note that flow occurs only if $(-\partial p/\partial x)^s > \tau_0 H$. The volumetric flow rate is given by

$$Q = \frac{2W}{3\mu}\left(-\frac{\partial p}{\partial x}\right)^s H^3\left[1-\frac{3}{2}\left(\frac{y_0}{H}\right)+\frac{1}{2}\left(\frac{y_0}{H}\right)^3\right], \tag{16}$$

where W is the width of the plates (in the z-direction).

We assume that at $t = 0$ the velocity $u_x(y,t)$ is given by the steady-state solution (14) and that at $t = 0^+$ the pressure gradient is reduced either to zero or to $(-\partial p/\partial x) < (-\partial p/\partial x)^s$, in which case the flow is expected to stop. The evolution of the velocity is again governed by the x-momentum equation. Using the same scales as in the plane Couette flow, with V denoting now the mean velocity in the slit, the dimensionless form of the x-momentum equation is obtained:

$$\frac{\partial u_x}{\partial t} = f + \frac{\partial \tau_{yx}}{\partial y}, \tag{17}$$

where f denotes the dimensionless pressure gradient. The dimensionless form of the constitutive equation is given by Eq. (7), and that of the steady velocity profile (14) is:

$$u_x^s(y) = \begin{cases} \frac{1}{2}f^s(1-y_0)^2, & 0 \le y \le y_0, \\ \frac{1}{2}f^s(1-y^2) - Bn(1-y), & y_0 \le y \le 1, \end{cases} \tag{18}$$

where

$$y_0 = \frac{Bn}{f^s} \tag{19}$$

and f^s is the dimensionless pressure gradient corresponding to $-(\partial p/\partial x)^s$. It turns out that y_0 is the real root of the cubic equation:

$$y_0^3 - 3\left(1+\frac{2}{Bn}\right)y_0 + 2 = 0. \tag{20}$$

It is clear that a steady flow in the channel occurs only if $f^s > Bn$. The dimensionless boundary and initial conditions for the time-dependent problem read:

$$\frac{\partial u_x}{\partial y}(0,t)=0, \quad t\geq 0, \qquad u_x(1,t)=0, \quad t\geq 0,$$
$$u_x(y,0)=u_x^s(y), \quad 0\leq y\leq 1. \tag{21}$$

In the case of Newtonian flow ($Bn = 0$), the time-dependent solution when the pressure gradient is suddenly reduced from f^s to f is given by [1]

$$u_x(y,t)=\frac{3}{2}\frac{f}{f^s}(1-y^2)+\frac{48}{\pi^3}\left(1-\frac{f}{f^s}\right)\sum_{k=1}^{\infty}\frac{(-1)^{k+1}}{(2k-1)^3} \times \cos\left[\frac{(2k-1)\pi}{2}y\right]\exp\left[-\frac{(2k-1)^2\pi^2}{4}t\right], \tag{22}$$

which indicates that the flow stops after an infinite amount of time only when $f = 0$. In the case of a Bingham plastic ($Bn > 0$), Huilgol et al. [3] provide the following upper bound for the stopping time:

$$T_f\leq\frac{4}{\pi^2}\ln\left[1+\frac{\pi^2}{4}\frac{\|u_x(y,0)\|}{Bn-f}\right], \quad f<Bn, \tag{23}$$

where $u_x(y,0)=u_x^s(y)$ is given by Eq. (18). The above bound is valid when $f < Bn$; otherwise, the flow will not stop.

3.3. Cessation of axisymmetric Poiseuille flow

The geometry of the axisymmetric Poiseuille flow is depicted in Fig. 1c. The steady-state solution for the ideal Bingham model is given by

$$u_z^s(r)=\begin{cases}\frac{1}{4\mu}\left(-\frac{\partial p}{\partial z}\right)^s(R-r_0)^2, & 0\leq r\leq r_0,\\ \frac{1}{4\mu}\left(-\frac{\partial p}{\partial z}\right)^s(R^2-r^2)-\frac{\tau_0}{\mu}(R-r), & r_0\leq r\leq R,\end{cases} \tag{24}$$

where $(-\partial p/\partial z)^s$ is the constant pressure gradient, and the yield point is given by

$$r_0=\frac{2\tau_0}{(-\partial p/\partial z)^s}<R. \tag{25}$$

The volumetric flow rate is given by

$$Q=\frac{\pi}{8\mu}\left(-\frac{\partial p}{\partial z}\right)^s R^4\left[1-\frac{4}{3}\left(\frac{r_0}{R}\right)+\frac{1}{3}\left(\frac{r_0}{R}\right)^4\right]. \tag{26}$$

We assume that at $t = 0$ the velocity $u_z(r,t)$ is given by the steady-state solution and that at $t = 0^+$ the pressure gradient is reduced either to zero or to $(-\partial p/\partial z) < (-\partial p/\partial z)^s$. Scaling the lengths by the tube radius R, the velocity by the mean velocity V, the pressure and the stress components by $\mu V/R$, and the time by $\rho R^2/\mu$, we obtain the dimensionless form of the z-momentum equation

$$\frac{\partial u_z}{\partial t}=f+\frac{1}{r}\frac{\partial}{\partial r}(r\tau_{rz}), \tag{27}$$

where f is the dimensionless pressure gradient. The dimensionless form of the constitutive equation is given by

$$\tau_{rz}=\left\{\frac{Bn[1-\exp(-M\dot\gamma)]}{\dot\gamma}+1\right\}\frac{\partial u_z}{\partial r}, \tag{28}$$

where $\dot\gamma=|\partial u_z/\partial r|$,

$$Bn\equiv\frac{\tau_0 R}{\mu V}, \tag{29}$$

and

$$M\equiv\frac{mV}{R}. \tag{30}$$

The steady velocity profile (24) takes the dimensionless form

$$u_z^s(r)=\begin{cases}\frac{1}{4}f^s(1-r_0)^2, & 0\leq r\leq r_0,\\ \frac{1}{4}f^s(1-r^2)-Bn(1-r), & r_0\leq r\leq 1,\end{cases} \tag{31}$$

where r_0 satisfies

$$r_0=\frac{2Bn}{f^s} \tag{32}$$

and f^s is the dimensionless pressure gradient corresponding to $-(\partial p/\partial z)^s$. We note that r_0 is a real root of:

$$r_0^4-4\left(1+\frac{3}{Bn}\right)r_0+3=0. \tag{33}$$

Clearly, a steady flow in the tube occurs only if $f^s > 2Bn$. The growth of r_0 with Bn is illustrated in Fig. 2, in which steady-state velocity profiles calculated for various Bingham numbers are shown.

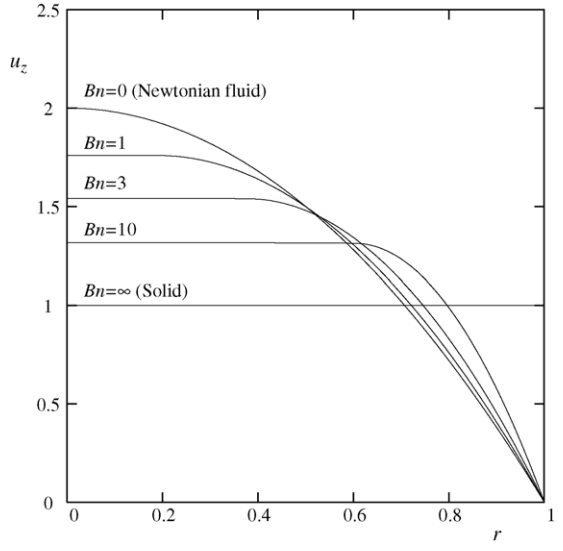

Fig. 2. Steady velocity distributions for various Bingham numbers in axisymmetric Poiseuille flow; $M = 200$.

The dimensionless boundary and initial conditions read:

$$\frac{\partial u_z}{\partial r}(0,t)=0, \quad t\geq 0, \qquad u_z(1,t)=0, \quad t\geq 0,$$
$$u_z(r,0)=u_z^s(r), \quad 0\leq r\leq 1. \tag{34}$$

The time-dependent solution for Newtonian flow ($Bn=0$), when the pressure gradient is suddenly reduced from f^s to f, is given by [1]

$$u_z(r,t)=2\frac{f}{f^s}(1-r^2)+16\left(1-\frac{f}{f^s}\right)\sum_{k=1}^{\infty}\frac{J_0(a_k r)}{a_k^3 J_1(a_k)}\,\mathrm{e}^{-a_k^2 t}, \tag{35}$$

where J_0 and J_1 are respectively the zeroth- and first-order Bessel functions of the first kind, and a_k, $k=1,2,\ldots$ are the roots of J_0. In the case of a Bingham plastic ($Bn>0$), Glowinski [2] provides the following upper bound for the stopping time:

$$T_f\leq\frac{1}{\lambda_1}\ln\left[1+\lambda_1\frac{\|u_z(r,0)\|}{2Bn-f}\right], \quad f<2Bn, \tag{36}$$

where $u_z(r,0)=u_z^s(r)$ is given by Eq. (31),

$$\|u_z(r,0)\|=\left[2\int_0^1 u_z^2(r,0)r\,\mathrm{d}r\right]^{1/2} \tag{37}$$

and λ_1 is the smallest (positive) eigenvalue of the problem:

$$\frac{1}{r}\frac{\mathrm{d}}{\mathrm{d}r}\left(r\frac{\mathrm{d}w}{\mathrm{d}r}\right)+\lambda w=0, \quad w'(0)=w(1)=0. \tag{38}$$

It is easily found that $\lambda_1=a_1^2\simeq 5.7831$, where a_1 is the least root of $J_0(x)$, with the corresponding eigenfunction being given by $w_1(x)=J_0(a_1x)$. Therefore,

$$T_f\leq\frac{1}{a_1^2}\ln\left[1+a_1^2\frac{\|u_z(r,0)\|}{2Bn-f}\right], \quad f<2Bn. \tag{39}$$

The bound (39) holds only when $f<2Bn$; otherwise, the flow will not stop.

4. Numerical results

Since there are no analytical solutions to the flows under study in the case of the Bingham plastic or the Papanastasiou model, we have used a numerical method, namely the finite element method with quadratic (P^2-C^0) elements for the velocity. For the spatial discretization, we used the Galerkin form of the momentum equation. For the time discretization, we used the standard fully-implicit (Euler backward-difference) scheme. At each time step, the nonlinear system of discretized equations was solved by using the Newton method. In the case of Couette flow, a 200-element mesh refined near the two plates has been used. In Poiseuille flows, the mesh consisted of 180 elements and was refined near the wall. Our numerical experiments with meshes of different refinement (ranging from 50 up to 400 elements) showed that the solutions obtained with the aforementioned optimal meshes are convergent. The effect of the time step has also been studied. In general, the time step should be reduced as the Bingham number or the regularization parameter M is increased, in order not only to ensure satisfactory accuracy but, more importantly, to ensure the convergence of the Newton–Raphson process which becomes very slow. In general, for $M=500$, the time step ranged from 10^{-4} ($Bn=0$) to 10^{-6} ($Bn=20$); these values were further reduced by the code whenever the Newton–Raphson process failed to converge. The code has also been tested by solving first the Newtonian flows and making comparisons with the analytical solutions. In all three problems, the agreement between the theory and the calculations was excellent.

4.1. Cessation of plane Couette flow

Figs. 3–5 show the evolution of the velocity for $Bn=0$ (Newtonian fluid), 2 and 20, respectively. The growth parameter has been taken to be $M=200$. The numerical solution in Fig. 3 compares very well with the analytical solution (11) for the Newtonian flow. The numerical solutions for Bingham flow (Figs. 4 and 5), show that a small unyielded region, where the velocity is flat, appears near the lower plate that moved prior to $t=0$. Note that for high Bingham numbers (i.e., $Bn>5$), very small time steps (of the order of 10^{-9}) were necessary in order to get convergence in the early stages of cessation. The size of the unyielded region increases as the time proceeds. Its left limit initially moves to the right but at higher times starts moving to the left, as the flow approaches complete cessation; see [4] for an explanation of this phenomenon.

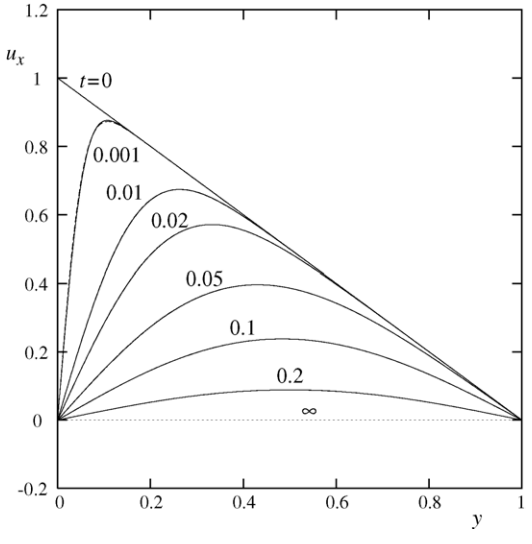

Fig. 3. Evolution of the velocity in cessation of plane Couette flow of a Newtonian fluid. Comparison of the analytical (solid lines) with the numerical (dashed lines) solutions.

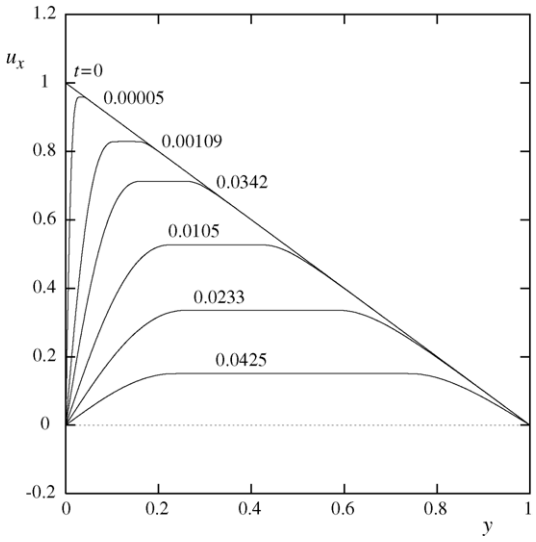

Fig. 4. Evolution of the velocity in cessation of plane Couette flow of a Bingham fluid with $Bn = 2$ and $M = 200$.

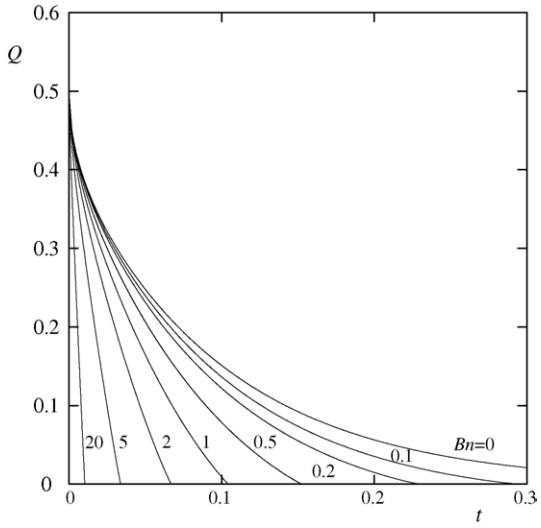

Fig. 6. Evolution of the volumetric flow rate during the cessation of plane Couette flow of a Bingham fluid with $M = 200$ and various Bingham numbers.

Fig. 6 shows the evolution of the volumetric flow rate,

$$Q(t) = \int_0^1 u_x(y, t)\,\mathrm{d}y, \tag{40}$$

for various Bingham numbers. These curves show the dramatic effect of the yield stress, which accelerates the cessation of the flow. In the Newtonian case ($Bn = 0$) and for small Bingham numbers the decay of the volumetric flow rate is exponential, at least initially. At higher Bingham numbers, the decay of Q becomes polynomial and eventually linear. The times at which $Q = 10^{-3}$ and 10^{-5} are plotted as functions of the Bingham number in Fig. 7. The two times coincide for moderate or large Bingham numbers, which indicates that the flow indeed stops at a finite time. In order to make comparisons with the theoretical upper bound (12), we consider the numerical stopping time as that when $Q = 10^{-5}$ is reached. As shown in Fig. 8, for moderate and higher Bingham numbers the numerical stopping time is just below the theoretical upper bound, which indicates that the latter is tight. The small discrepancies observed for low Bingham numbers are due to the fact that the value of the regularization parameter M is not sufficiently high. For very small Bn, the effect of M is not crucial, since the material is practically Newtonian, which explains why the numerical stopping time falls again below the theoretical upper bound, as it should. The effect of M is discussed in more detail in the case of the plane Poiseuille flow.

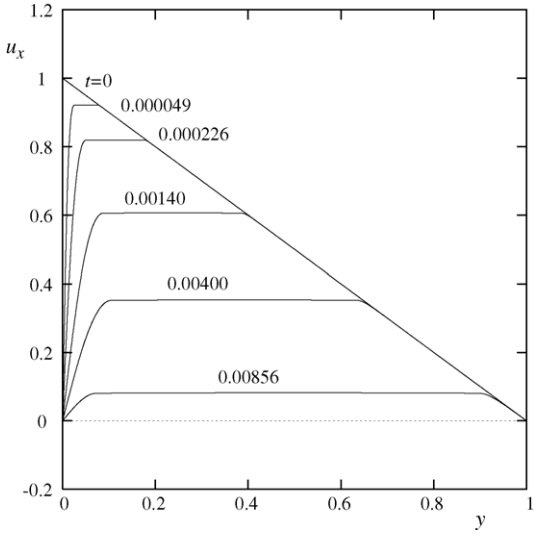

Fig. 5. Evolution of the velocity in cessation of plane Couette flow of a Bingham fluid with $Bn = 20$ and $M = 200$.

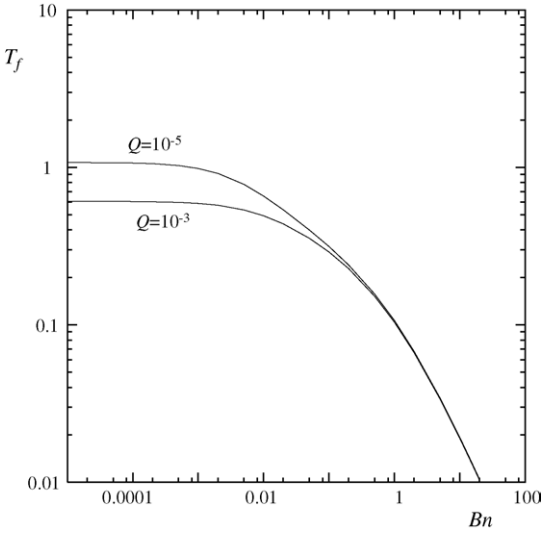

Fig. 7. Calculated times for $Q = 10^{-3}$ and 10^{-5} in cessation of plane Couette flow of a Bingham fluid with $M = 200$.

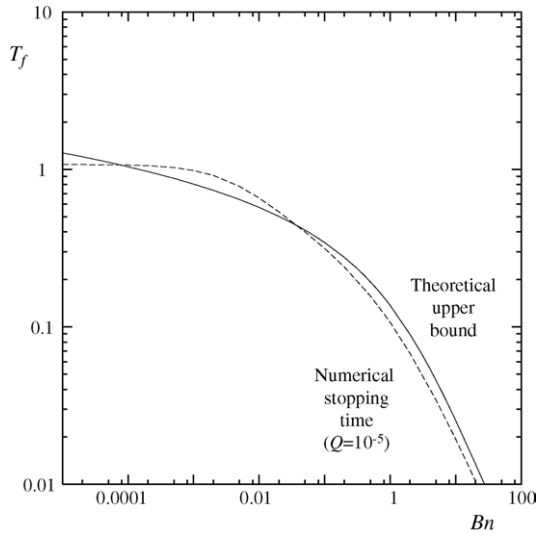

Fig. 8. Comparison of the computed stopping time ($Q = 10^{-5}$) in cessation of plane Couette flow of a Bingham fluid with the theoretical upper bound (12); $M = 200$.

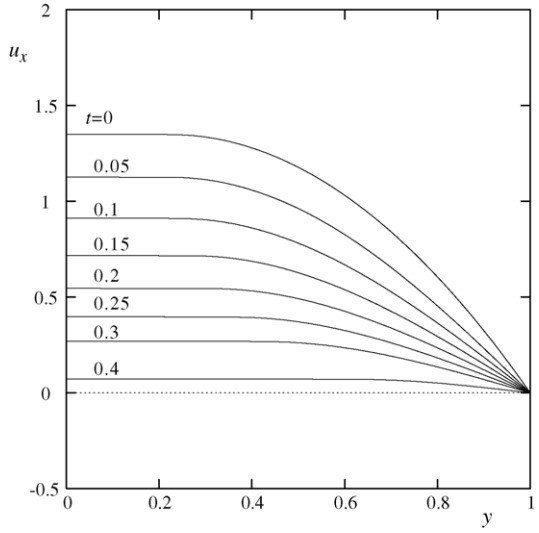

Fig. 10. Evolution of the velocity in cessation of plane Poiseuille flow of a Bingham fluid with $Bn = 1$ and $M = 200$.

4.2. Cessation of plane Poiseuille flow

Figs. 9–12 show the evolution of $u_x(y, t)$ for $Bn = 0$ (Newtonian case), 1, 5 and 20. In Fig. 13, we see the evolution of the calculated volumetric flow rate for various Bingham numbers. As in plane Couette flow, the decay of the volumetric flow rate is almost exponential for small Bingham numbers and becomes polynomial at higher Bn values. Fig. 14 shows plots of the times required for the volumetric flow rate to become 10^{-3} and 10^{-5} versus the Bingham number for both plane and axisymmetric Poiseuille flows (with $M = 200$).

Before proceeding to the comparisons with the theoretical upper bound (23), let us investigate the effect of the growth parameter M on the calculated stopping times. As demonstrated in Fig. 15, which shows the results obtained with $M = 200$ and 500, the calculated stopping times are not so sensitive to M when the Bingham number is moderate or high, i.e. $Bn \geq 1$. For smaller Bingham numbers, i.e. $10^{-3} \leq Bn \leq 1$, the time required for the volumetric flow rate to become 10^{-5} is reduced as M is increased. For very small Bingham numbers, the fluid is essentially Newtonian, and therefore the value of M has no effect on the calculations. Hence, in order to get convergent results in the range $10^{-3} \leq Bn \leq 1$, the value of M has to be increased further. However, our studies showed that when $M = 1000$, convergence difficulties are observed when $Bn > 0.01$. Reducing the time step might extend the calculations to a slightly higher Bn, but beyond a critical Bn value the required time step becomes very small and the accumulated round-off errors

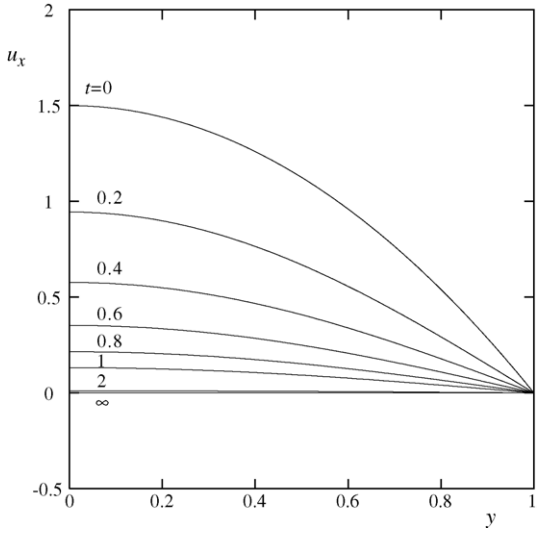

Fig. 9. Evolution of the velocity in cessation of plane Poiseuille flow of a Newtonian fluid.

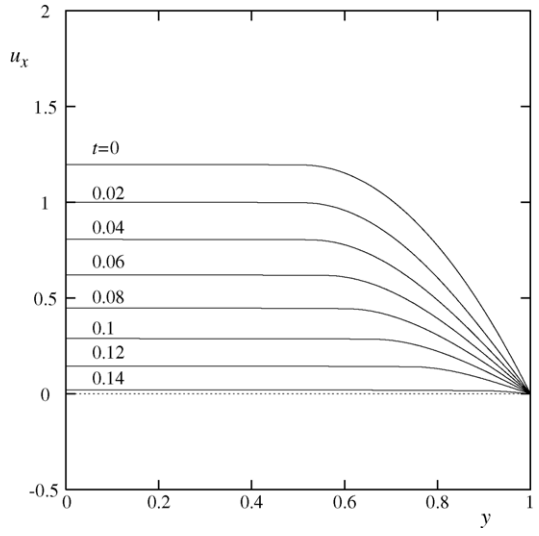

Fig. 11. Evolution of the velocity in cessation of plane Poiseuille flow of a Bingham fluid with $Bn = 5$ and $M = 200$.

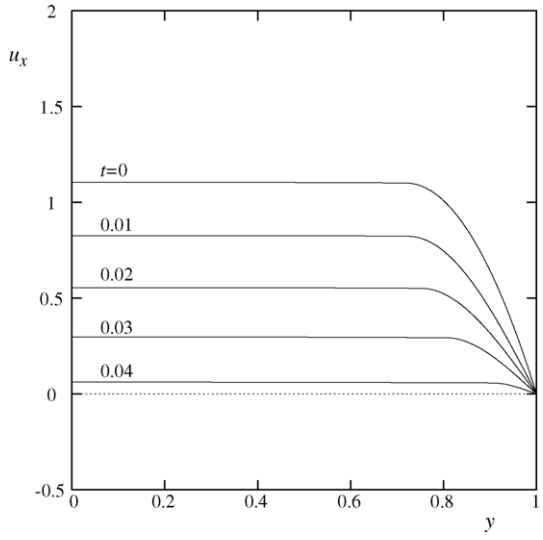

Fig. 12. Evolution of the velocity in cessation of plane Poiseuille flow of a Bingham fluid with $Bn = 20$ and $M = 200$.

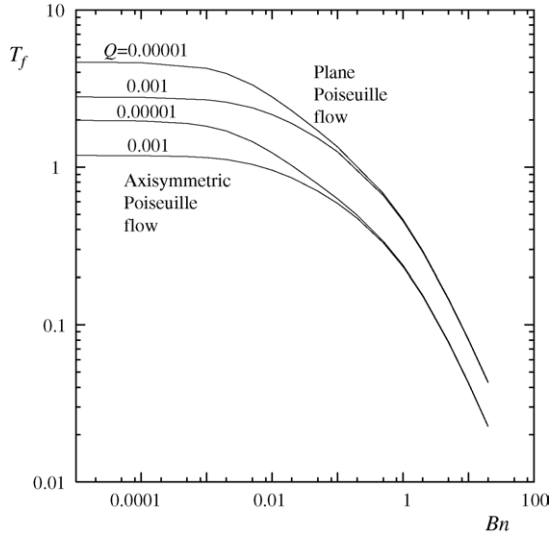

Fig. 14. Calculated times for $Q = 10^{-3}$ and 10^{-5} in cessation of plane and axisymmetric Poiseuille flows of Bingham fluids with $M = 200$.

are so high so that the error in the calculated stopping time is higher than that corresponding to a smaller value of M. As a conclusion, decreasing the time step is not the best way to obtain good results for $M > 500$. If results for small (but not vanishingly small) Bingham numbers and large M are necessary, then continuation in M must be used at each time step. According to our numerical experiments, using such a continuation will increase the computational time by at least 10 times. Since we are not interested in such small values of Bn, such calculations have not been pursued.

A comparison between theory and calculations is provided in Fig. 16 for the case $f = 0$ (i.e., when the imposed pressure gradient is set to zero). Again, the computed stopping time is just below the theoretical upper bound (23) for moderate and high Bingham numbers. The small discrepancies observed for small values of the Bingham number are due to the fact that M is not sufficiently high. We have also examined the case in which the imposed pressure gradient f is not zero. An ideal Bingham plastic stops after a finite time if $f \leq Bn$ and reaches a new steady-state if $f > Bn$ (with the volumetric flow rate corresponding to the new value of f). This is not the case with a regularized Bingham fluid. Since M is finite, the flow will reach a new steady-state in which the volumetric flow rate may be small but not zero. To illustrate this effect, we considered the case in which $Bn = 1$ and $M = 500$ and carried out simulations for different values of f. In Fig. 17a, we see the evolution of the volumetric flow rate for different values of f. Fig. 17b is a zoom of the previous figure showing that indeed the volumetric flow rate reaches a

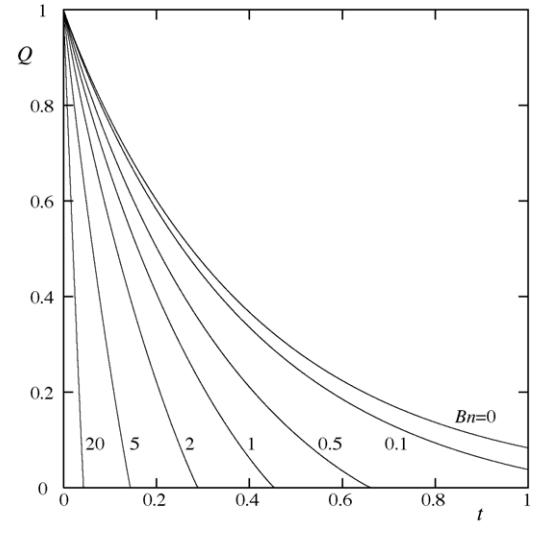

Fig. 13. Evolution of the volumetric flow rate during the cessation of plane Poiseuille flow of a Bingham fluid with $M = 200$ and various Bingham numbers.

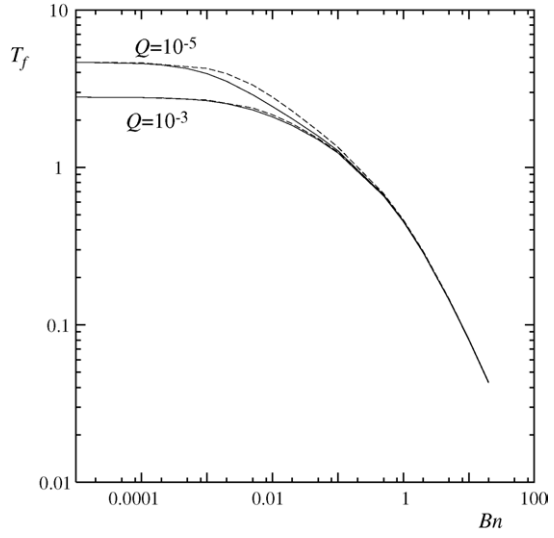

Fig. 15. Calculated times for $Q = 10^{-3}$ and 10^{-5} in cessation of plane Poiseuille flow of Bingham fluids with $M = 200$ (dashed) and $M = 500$ (solid).

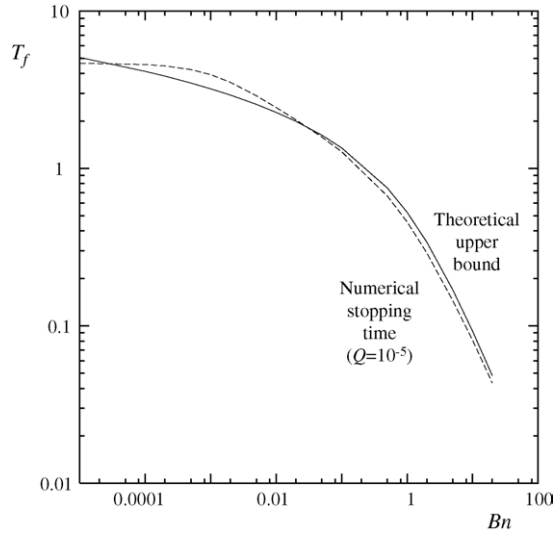

Fig. 16. Comparison of the computed stopping time ($Q = 10^{-5}$) in cessation of plane Poiseuille flow of a Bingham fluid with the theoretical upper bound (23); $f = 0$ and $M = 500$.

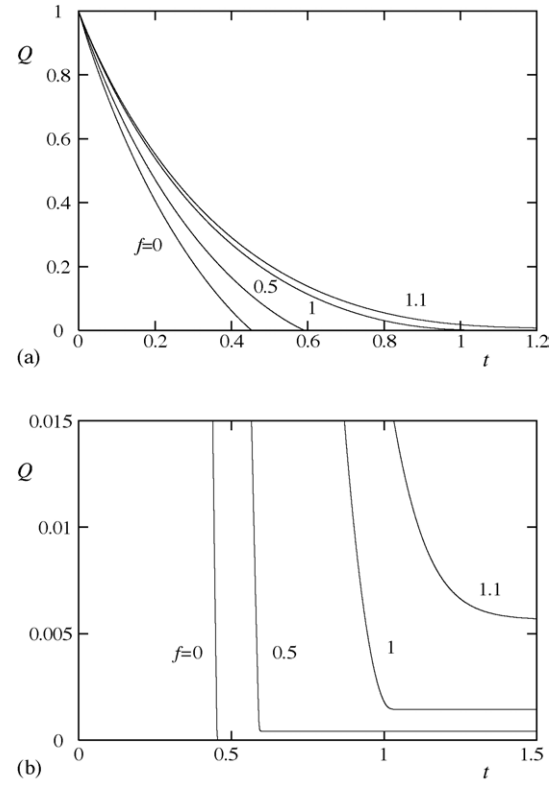

Fig. 17. (a) Evolution of the volumetric flow rate for various values of the imposed pressure gradient f; (b) detail of the same plot showing that a finite volumetric flow rate is reached when $f > 0$; plane Poiseuille flow with $Bn = 1$ and $M = 500$.

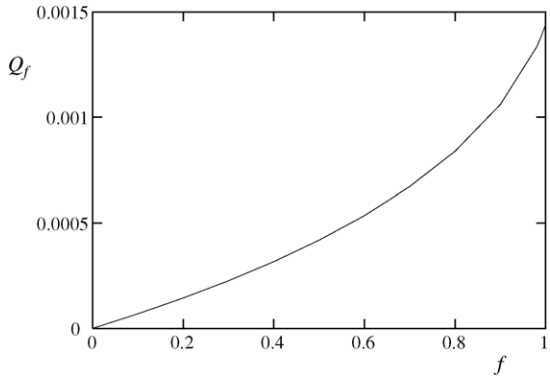

Fig. 18. Volumetric flow rates reached with the regularized Papanastasiou model vs. the imposed pressure gradient f; plane Poiseuille flow, $Bn = 1$ and $M = 500$.

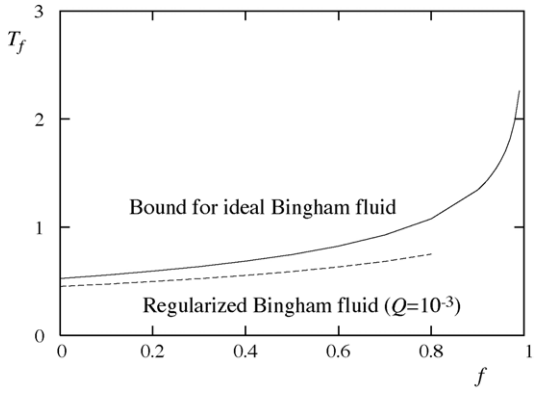

Fig. 19. Comparison of the times required to reach $Q = 10^{-3}$ in cessation of plane Poiseuille flow of a regularized Bingham fluid with the theoretical upper bound (23) for an ideal Bingham fluid; $Bn = 1$ and $M = 500$.

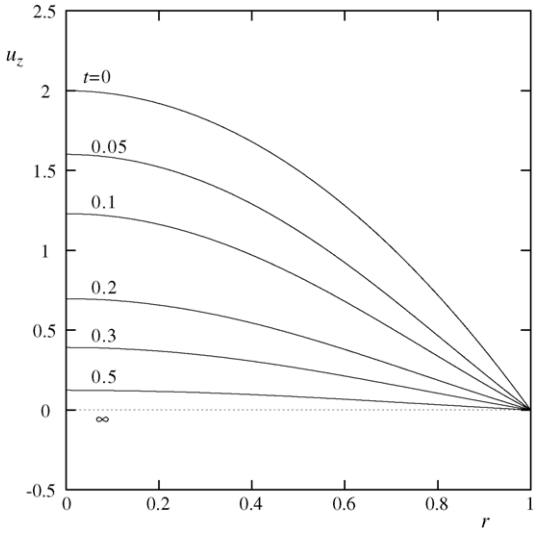

Fig. 20. Evolution of the velocity in cessation of axisymmetric Poiseuille flow of a Newtonian fluid.

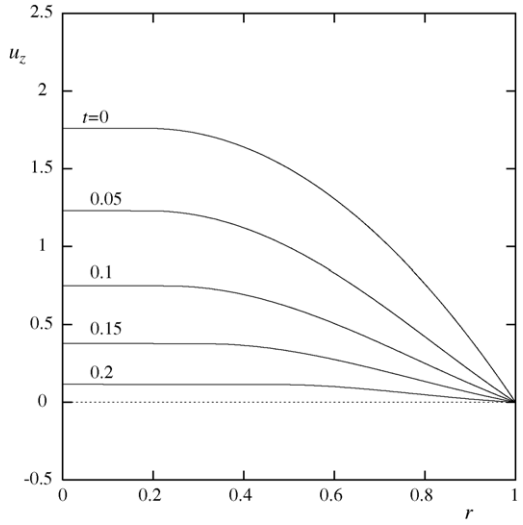

Fig. 21. Evolution of the velocity in cessation of axisymmetric Poiseuille flow of a Bingham fluid with $Bn = 1$ and $M = 200$.

finite value when $f \neq 0$. This value may be reduced further by increasing the value of M. The new volumetric flow rate is plotted against f in Fig. 18. Finally, in Fig. 19 we compare the times required to reach $Q = 10^{-3}$ with the theoretical upper bound (23). For smaller values of Q, the numerical results move closer to the theoretical upper bound, but in a smaller range of f, which is easily deduced from Fig. 18. The deviations between the theoretical predictions and the numerical solutions become larger as the value of the imposed pressure gradient is increased. These, however, can be further reduced by increasing the value of M.

4.3. Cessation of axisymmetric Poiseuille flow

The results for the axisymmetric Poiseuille flow are very similar to those obtained for the planar case. Figs. 20–23

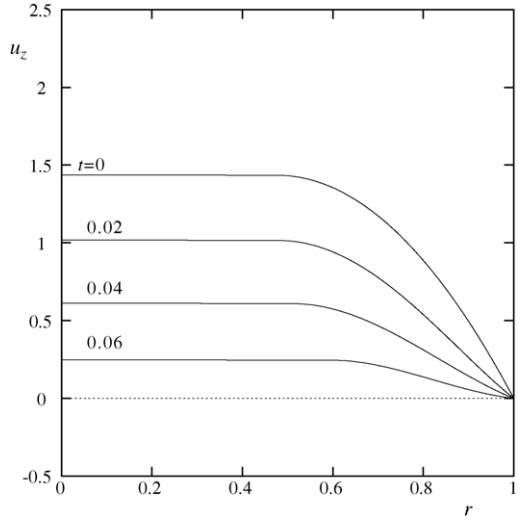

Fig. 22. Evolution of the velocity in cessation of axisymmetric Poiseuille flow of a Bingham fluid with $Bn = 5$ and $M = 200$.

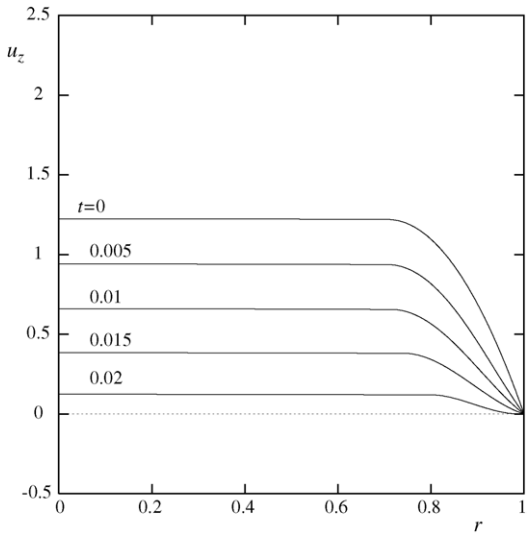

Fig. 23. Evolution of the velocity in cessation of axisymmetric Poiseuille flow of a Bingham fluid with $Bn = 20$ and $M = 200$.

show the evolution of u_z for $M = 200$ and $Bn = 0$ (Newtonian case), 1, 5 and 20. Fig. 24 shows in detail how the velocity profile changes near the wall when $Bn = 20$. A second unyielded region of a smaller size appears near the wall, in which the velocity is zero. The growth of this region cannot be explained physically and is considered as a numerical artifact due to the regularization of the constitutive equation.

In Fig. 25, we see the evolution of the calculated volumetric flow rate (scaled by 2π),

$$Q(t) = \int_0^1 u_z(r, t) r \, \mathrm{d}r, \tag{41}$$

for $M = 200$ and various Bingham numbers. As in plane Poiseuille flow, the cessation of the flow is accelerated as the

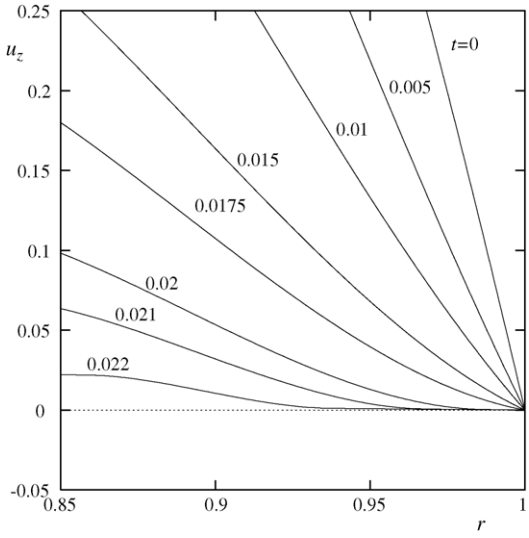

Fig. 24. Detail near the wall of the evolution of the velocity in cessation of axisymmetric Poiseuille flow of a Bingham fluid with $Bn = 20$ and $M = 200$.

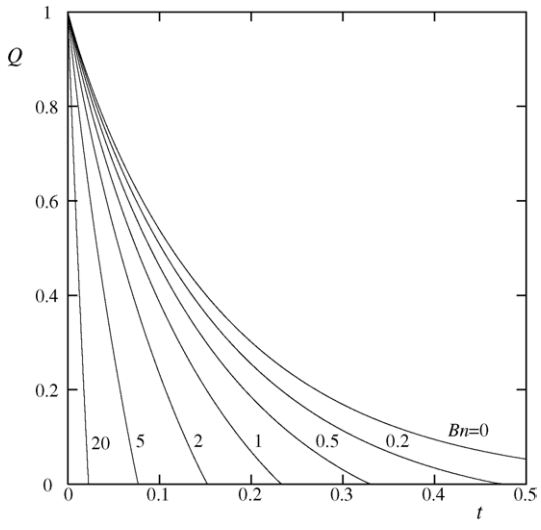

Fig. 25. Evolution of the volumetric flow rate during the cessation of axisymmetric Poiseuille flow of a Bingham fluid with $M = 200$ and various Bingham numbers.

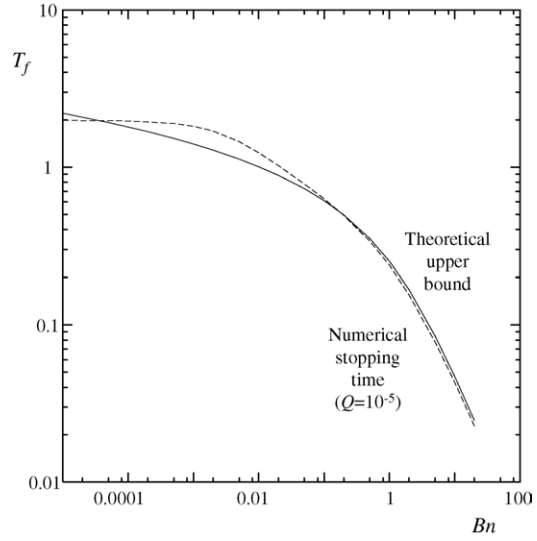

Fig. 26. Comparison of the computed stopping time ($Q = 10^{-5}$) in cessation of axisymmetric Poiseuille flow of a Bingham fluid with the theoretical upper bound (39); $f = 0$ and $M = 500$.

Bingham number is increased. The calculated stopping times for $Q = 10^{-5}$ and $f = 0$, plotted versus the Bingham number in Fig. 26, agree well with the theoretical upper bound (39), with the small discrepancies observed for low *Bn* as expected.

5. Conclusions

The Papanastasiou modification of the Bingham model has been employed in order to solve numerically the cessation of plane Couette, plane Poiseuille, and axisymmetric Poiseuille flows of a Bingham plastic. The finite element calculations showed that the volumetric flow rate decreases exponentially for low, polynomially for moderate, and linearly for high Bingham numbers. Unlike their counterparts in a Newtonian fluid, the corresponding times for complete cessation are finite, in agreement with theory. The numerical stopping times are found to be in very good agreement with the theoretical upper bounds provided in Refs. [2,3], for moderate and higher Bingham numbers. Some minor discrepancies observed for rather low Bingham numbers can be reduced by increasing the regularization parameter introduced by the Papanastasiou model.

A noteworthy difference between the predictions of the ideal and the regularized Bingham model is revealed when the imposed pressure gradient is nonzero and below the critical value at which a nonzero steady-state Poiseuille solution exists. In contrast with the ideal Bingham flow which reaches cessation in a finite time, the regularized flow reaches a steady velocity profile corresponding to a small but nonzero volumetric flow rate. The value of the latter may be reduced by increasing the value of the regularization parameter *M* but will always be nonzero.

Acknowledgements

Part of this research is supported by the "HERAKLEITOS" program of the Ministry of Education and Religious Affairs of Greece (#68/0655). The project is co-funded by the European Social Fund (75%) and National Resources (25%). This research was also partially supported by the Research Committee of the University of Cyprus. Financial support from the program "SOCRATES" for scientific exchanges between Greece and Cyprus is gratefully acknowledged.

References

[1] T. Papanastasiou, G. Georgiou, A. Alexandrou, Viscous Fluid Flow, CRC Press, Boca Raton, 1999.
[2] R. Glowinski, Numerical Methods for Nonlinear Variational Problems, Springer-Verlag, New York, 1984.
[3] R.R. Huilgol, B. Mena, J.M. Piau, Finite stopping time problems and rheometry of Bingham fluids, J. Non-Newtonian Fluid Mech. 102 (2002) 97.
[4] R.R. Huilgol, On kinematic conditions affecting the existence and non-existence of a moving yield surface in unsteady unidirectional flows of Bingham fluids, J. Non-Newtonian Fluid Mech. 123 (2004) 215.
[5] R.R. Huilgol, Variational inequalities in the flows of yield stress fluids including inertia: theory and applications, Phys. Fluids 14 (2002) 1269.
[6] T.C. Papanastasiou, Flows of materials with yield, J. Rheol. 31 (1987) 385.
[7] M. Chatzimina, G.C. Georgiou, E. Mitsoulis, R.R. Huilgol, Finite stopping times in Couette and Poiseuille flows of viscoplastic fluids, in: Proceedings of the XIVth International Congress on Rheology, Seoul, Korea, pp. NFF22-1–NFF22-4, 2004.
[8] Y. Dimakopoulos, J. Tsamopoulos, Transient displacement of a viscoplastic material by air in straight and suddenly constricted tubes, J. Non-Newtonian Fluid Mech. 112 (2003) 43.
[9] E. Mitsoulis, R.R. Huilgol, Entry flows of Bingham plastics in expansions, J. Non-Newtonian Fluid Mech. 122 (2004) 45.